

Anisotropy of the Electron Momentum Distribution in Pyrolytic Graphite Studied Using a $WK\alpha_1$ Spectrometer*

S. Manninen and V. Honkimäki

University of Helsinki, Department of Physics, Helsinki, Finland

P. Suortti

ESRF, B.P. 220, F-38043 Grenoble, France

Z. Naturforsch. **48a**, 295–298 (1993); received December 12, 1991

A new spectrometer construction based on a high-voltage W-anode x-ray tube has been used to measure the directional Compton profiles of a pyrolytic graphite crystal. Owing to the focusing geometry, the monochromatic $WK\alpha_1$ beam is very well collimated, which improves the momentum resolution compared with conventional ^{241}Am spectrometers, operated almost at the same energy. The experimental anisotropy in the basal plane and in the direction of the c -axis is found to be very close to that of a recent calculation, based on the pseudopotential local-density-functional model.

Key words: Compton profile; Pyrolytic graphite; $WK\alpha_1$ -spectrometer; Focusing monochromator; Autocorrelation function.

1. Introduction

The renaissance of Compton scattering experiments in the 1960's was based on the use of crystal spectrometers to analyse the energy spectrum of the scattered radiation [1]. The relatively low power of the x-ray tubes combined with the non-focusing crystal optics led to the period when various gamma-ray sources were the main tools in momentum density studies [2–7]. Depending on the gamma-ray energy, the momentum resolution obtained using a solid state detector varied within 0.4–0.6 a.u. of momentum. In the 1980's, several reasons to reconsider the experimental improvements were found: (i) The x-ray flux available at the synchrotron laboratories was several orders of magnitude larger than what could be obtained from conventional sources. Also the development of the x-ray tubes made it possible to design focusing crystal spectrometers for inelastic scattering studies [8]. (ii) The momentum resolution obtained using gamma-ray sources and solid-state detectors was not good

enough to make detailed comparisons with the state-of-the-art band structure calculations. This was not only because of the resolution limitation of the solid-state detector, but inelastic scattering in the gamma-ray source gives additional impurity and the angular divergences owing to the size of the source give additional momentum broadening. Moreover, in the case of an annular source the direction of the scattering vector is not well defined. (iii) The rapid development in the detector technology gave several alternatives to improve both the momentum resolution and counting statistics [9–11].

In this work we describe a momentum density study of pyrolytic graphite, performed using a spectrometer based on 59.3 keV $WK\alpha_1$ radiation obtained using a focusing monochromator. Although the scattered radiation is analyzed with a solid-state detector, improvements compared with the gamma-ray spectrometers working at the same energy include well-defined beam and monochromatic primary energy without the problem of inelastic scattering in the source.

Pyrolytic graphite was chosen as a sample because it has been studied using various types of x-ray and gamma-ray spectrometers [12–16]. The performance of the present spectrometer can be therefore compared with the previous ones. Also there are number of calculations based on different models on the pyrolytic graphite crystal.

* Presented at the Sagamore X Conference on Charge, Spin, and Momentum Densities, Konstanz, Fed. Rep. of Germany, September 1–7, 1991.

Reprint requests to Dr. S. Manninen, University of Helsinki, Department of Physics, Siltavuorenpenger 20D, SF-00170 Helsinki, Finland/Suomi.

0932-0784 / 93 / 0100-0295 \$ 01.30/0. – Please order a reprint rather than making your own copy.



Dieses Werk wurde im Jahr 2013 vom Verlag Zeitschrift für Naturforschung in Zusammenarbeit mit der Max-Planck-Gesellschaft zur Förderung der Wissenschaften e.V. digitalisiert und unter folgender Lizenz veröffentlicht: Creative Commons Namensnennung-Keine Bearbeitung 3.0 Deutschland Lizenz.

Zum 01.01.2015 ist eine Anpassung der Lizenzbedingungen (Entfall der Creative Commons Lizenzbedingung „Keine Bearbeitung“) beabsichtigt, um eine Nachnutzung auch im Rahmen zukünftiger wissenschaftlicher Nutzungsformen zu ermöglichen.

This work has been digitalized and published in 2013 by Verlag Zeitschrift für Naturforschung in cooperation with the Max Planck Society for the Advancement of Science under a Creative Commons Attribution-NoDerivs 3.0 Germany License.

On 01.01.2015 it is planned to change the License Conditions (the removal of the Creative Commons License condition “no derivative works”). This is to allow reuse in the area of future scientific usage.

2. Experimental

The detailed description of the spectrometer is published elsewhere [17] and only a brief summary is given here. The x-ray source is a sealed tube with W-target. The maximum voltage is 160 kV, and the maximum loading with the fine focus is 700 W. The take-off angle of radiation (the angle between the anode surface and the center line of the x-ray beam) can be adjusted between 4° and 39° degrees by moving the slit/shutter assembly in front of the tube window. The corresponding optical width of the tube focus is from 0.07 mm to 0.67 mm. This should be matched with the width of the reflectivity curve of the symmetrically cut Ge(400) monochromator crystal. Taking into account the absorption in the tube anode, a compromise to the optical width of 0.22 mm was made. The beam after the monochromator was measured using a small pin-hole in front of the Ge detector; no trace of $\text{WK}\alpha_2$ was obtained. In addition, the low-energy tail, which is typical for the gamma-ray sources, turned out to be negligible.

The monochromatic flux of $\text{WK}\alpha_1$ -photons was determined by measuring the integrated intensities of Bragg reflections from a standard powder sample and was found to be about 10^7 photons/s. It agrees well with the calculation, based on the measurement of the flux of characteristic x-rays [18]. Because the beam size at the sample position is about 15 mm high and 0.5 mm wide, this means that compared with a typical ^{241}Am -spectrometer, where a beam size of the order of 1 cm^2 is used, much smaller samples can be studied with the same statistical accuracy. Especially in the case of needle-like crystals the full beam size can be utilized.

The scattering angle in the spectrometer can be changed. This makes it possible to study, for example, the inelastic scattering cross-section as a function of the momentum transfer. Also coincidence experiments in which the inner-shell contribution to inelastic scattering is separated by detecting x-ray fluorescence in coincidence with the scattered photon, are much easier to carry out than similar measurements using gamma-ray sources. Here the main advantages are (i) a well-collimated beam, which improves the momentum resolution, and (ii) the removal of constraints arising from the size of the gamma-ray source and shielding in the two-detector geometry (both detectors and the source should be located close to the sample to maximize the low coincidence counting rate). In Compton-

profile experiments the scattering angle should be as large as possible; it is 160° in the present spectrometer. The peak of the profile is then at the energy of 48.5 keV. Using a high-quality solid-state detector, the energy resolution at that energy is about 335 eV and combined with the angular divergence effect, which is almost totally due to the finite size of the detector crystal, the total momentum resolution is close to 0.5 a.u.

The pyrolytic graphite sample was specially cut for the experiment. In order to keep the scattering geometry unchanged, the cross-section was a square (5×5) mm^2 , and the height of the crystal was 20 mm. Measurements with the scattering vector parallel to the *c*-axis and perpendicular to it could be done by a 90° rotation of the crystal. Most of the factors affecting the scattered intensity then cancel out when the directional momentum distribution differences are considered. This is very important, because the anisotropy effects are always small, typically of the order of one per cent.

During the measuring period of 80 000 s, about 170 000 counts were collected at the Compton peak channel (width 0.1 a.u.) for both crystal directions. A separate background measurement was made using the sample holder in the evacuated scattering chamber; the peak-to-background ratio turned out to be about 1000:1. The data were corrected for the energy-dependent effects (absorption, cross-section) and deconvoluted using a resolution function obtained from the direct-beam measurement. The total double/single scattering ratio was calculated using a Monte Carlo simulation program [19] and it was about 12%.

3. Results and Discussion

The final experimental Compton profiles and the difference $J(p_z)_{\text{c-ax}} - J(p_z)_{\text{bas}}$ are given in Table 1. Also shown is a recent calculation, based on a pseudo-potential within a local-density-functional model [20]. The 1s contribution has been added to the theoretical profiles, and they have been convoluted with the residual resolution function. As can be seen, the agreement with the experimental and theoretical Compton profiles is good, but there are small differences larger than the quoted statistical error. The main reason for this is due to the use of the pseudo-wave-functions, which do not have oscillations close to the nuclei leading to the omission of high-momentum components [20].

Table 1. The experimental and theoretical [20] Compton profiles of graphite, measured using the W-spectrometer. The 1s contribution has been added to the theoretical profiles and they have been convoluted with the residual instrument function of the experiment. The experimental error (including the statistical error and the uncertainty due to the deconvolution) is given at some points. The experimental and theoretical Compton-profile anisotropies ($\Delta J = J(p_z)_{c\text{-ax}} - J(p_z)_{\text{bas}}$) are also given.

p_z	c -axis (exp)	c -axis (th)	basal (exp)	basal (th)	ΔJ_{exp}	ΔJ_{th}
0.0	2.166 ± 0.016	2.250	2.197	2.301	-0.084	-0.104
0.1	2.154	2.244	2.183	2.291	-0.070	-0.108
0.2	2.127	2.222	2.149	2.258	-0.095	-0.109
0.3	2.081	2.183	2.092	2.200	-0.102	-0.108
0.4	2.014	2.117	2.011	2.119	-0.103	-0.108
0.5	1.920	2.018	1.907	2.006	-0.098	-0.099
0.6	1.800	1.889	1.781	1.871	-0.089	-0.090
0.7	1.652	1.727	1.637	1.715	-0.075	-0.078
0.8	1.485	1.544	1.481	1.547	-0.059	-0.066
0.9	1.305	1.348	1.321	1.373	-0.043	-0.052
1.0	1.127 ± 0.011	1.157	1.163	1.203	-0.030	-0.040
1.2	0.812	0.827	0.869	0.886	-0.015	-0.017
1.4	0.594	0.600	0.627	0.621	-0.006	-0.006
1.6	0.467	0.465	0.452	0.431	0.002	0.021
1.8	0.388	0.372	0.345	0.313	0.016	0.032
2.0	0.330 ± 0.006	0.305	0.291	0.258	0.025	0.033
3.0	0.176	0.155	0.174	0.155	0.021	0.019
4.0	0.100	0.088	0.104	0.090	0.012	0.014
5.0	0.057 ± 0.003	0.052	0.060	0.052	0.005	0.008

This effect as well as the experimental uncertainties mostly cancel out when the difference is taken, and as can be seen in Table 1, the agreement between the experimental and theoretical difference curves is excellent.

A more detailed analysis of the experimental and theoretical data can be done in terms of the autocorrelation function $B(z)$, obtained from the Compton profile $J(p_z)$ via Fourier transformation,

$$B(z) = \int_{-\infty}^{+\infty} J(p_z) \exp\{-ip_z z\} dp_z. \quad (1)$$

One of the main advantages in using $B(z)$ is that it is a position-space function and then allows direct comparison with quantities like the chemical bond and lattice spacings. In the case of semiconductors and insulators, $B(z)$ must have zeros at the lattice vectors.

The theoretical $B(z)$ -functions, based on the pseudopotential local-density-functional model [20], are shown in Figure 1. Comparison between the theory and the experiment should not be done until the resolution effects have been taken into account. Figures 2 and 3 show both the experimental results and the theoretical ones after the resolution damping (the res-

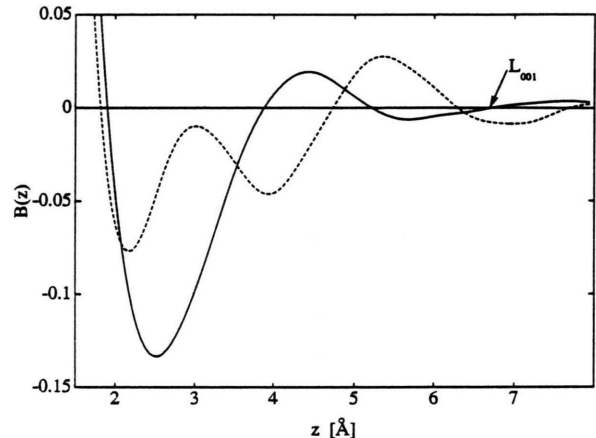


Fig. 1. Theoretical $B(z)$ functions of the pyrolytic graphite parallel to the c -axis (solid line) and in the basal plane. The length of the c -axis (6.696 Å) is shown by the arrow.

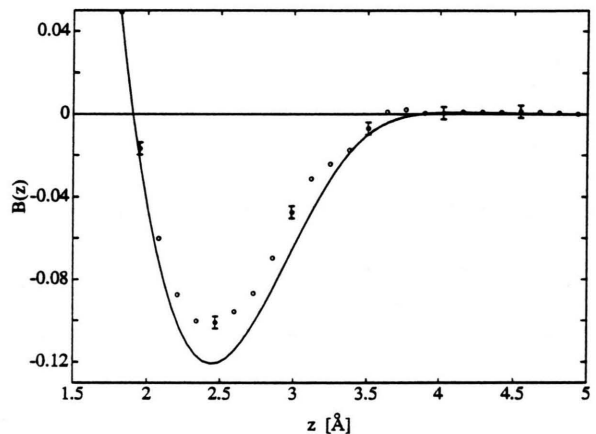


Fig. 2. Experimental and theoretical (solid line) $B(z)$ functions, calculated parallel to the c -axis. The resolution effect is included in the theory. The statistical error is given at some points.

olution broadening in the momentum space is well approximated as a convolution with a Gaussian function, leading to a multiplicative damping in the position space). This limits the position information to $z \leq 5$ Å. Although the amplitudes of the $B(z)$ -oscillations are somewhat different in experiment and theory, the general behaviour is the same. Interpreted in terms of the graphite lattice, some conclusions can be drawn.

(i) The length of the c -axis in graphite is 6.696 Å and it is therefore too far out to be seen experimentally as a zero of $B(z)$. On the other hand, the calculation has a zero at the right position, as seen in Figure 1. There

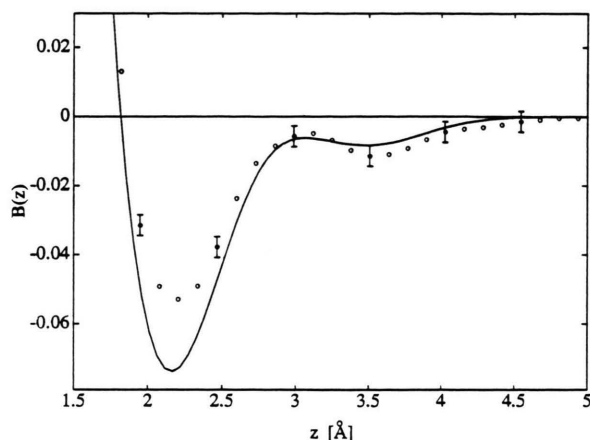


Fig. 3. Experimental and theoretical $B(z)$ functions, calculated at the basal plane. The resolution effect is included in the theory. The statistical error is given at some points.

is only cylindrical symmetry in the basal plane of the pyrolytic crystal and therefore the analysis based on the zero positions is more uncertain. In an earlier work [14] a detailed analysis of $B(z)$ in terms of the experimental and theoretical data is given.

(ii) The close agreement of experiment and theory, both in terms of the Compton-profile anisotropy and the $B(z)$ -function, shows that the electron momentum density in pyrolytic graphite is well understood. The next step would be a measurement on a graphite single crystal. The calculated momentum density [20, 21] could then be compared with the experimental result, which can be constructed using measured directional

Compton profiles. Unfortunately, such a crystal with sufficiently large dimensions does not exist at the moment.

Compared with the other calculations (molecular orbitals, pseudopotential [13], tight binding [14]) the pseudopotential within the local-density scheme [20] seems to give a much better description of the electronic structure of pyrolytic graphite. This is mostly due to the fact that the interlayer interaction has not been properly included in the previous models. Even the recent pseudopotential result [21] does not agree with the experimental data. The earlier experiments [12–16] are all in qualitative agreement with the present data, but there are differences, partly due to the omission of the multiple-scattering correction and/or to the nonconstant sample geometry.

This work shows that conventional solid-state-detector spectroscopy can be used in momentum density anisotropy studies, provided the other factors affecting the momentum resolution (geometrical divergences, sample geometry, deconvolution) are optimized. The small beam size in the present spectrometer additionally allows studies on small crystals, completely out of question with conventional γ -sources.

Acknowledgements

The authors wish to thank Riitta Karhumaa, M.Sc., for helping in data processing. They also acknowledge the financial support from the Academy of Finland.

- [1] M. J. Cooper, J. A. Leake, and R. J. Weiss, *Phil. Mag.* **12**, 797 (1965).
- [2] J. Felsteiner, R. Fox, and S. Kahane, *Phys. Lett.* **33 A**, 442 (1970).
- [3] P. Eisenberger and W. A. Reed, *Phys. Rev. A* **5**, 2085 (1972).
- [4] W. Weyrich, *Ber. Bunsenges. Phys. Chem.* **79**, 1085 (1975).
- [5] S. Manninen and T. Paakkari, *Nucl. Instrum. Meth.* **155**, 115 (1978).
- [6] R. S. Holt, M. Cooper, J. L. Du Bard, J. B. Forsyth, T. L. Jones, and K. Knights, *J. Phys. E: Sci. Instrum.* **12**, 1148 (1979).
- [7] P. Pattison and J. R. Schneider, *Nucl. Instrum. Meth.* **158**, 145 (1979).
- [8] P. Suortti, P. Pattison, and W. Weyrich, *J. Appl. Cryst.* **19**, 336, 342; P. Pattison, P. Suortti, and W. Weyrich, *ibid.* **19**, 353 (1986).
- [9] G. Loupiau and J. Petiau, *J. Physique* **41**, 265 (1980).
- [10] N. Shiotani, N. Sakai, F. Itoh, M. Sakurai, H. Kawata, Y. Amemiya, and M. Ando, *Nucl. Instrum. Meth. A* **275**, 447 (1989).
- [11] N. Sakai, N. Shiotani, M. Ito, F. Itoh, H. Kawata, Y. Amemiya, and M. Ando, *Rev. Sci. Instrum.* **60**, 1666 (1989).
- [12] T. L. P. Paakkari, *Phys. Fenn.* **9**, 185 (1974).
- [13] W. A. Reed, P. Eisenberger, K. C. Pandey, and L. C. Snyder, *Phys. Rev. B* **10**, 1507 (1974).
- [14] S. Vasudevan, T. Rayment, B. G. Williams and R. S. Holt, *Proc. Roy. Soc. A* **391**, 109 (1984).
- [15] G. Loupiau, J. Chomilier, and J. Guerard, *Solid State Commun.* **55**, 299 (1985).
- [16] R. Tyk, J. Felsteiner, I. Gertner, and R. Moreh, *Phys. Rev. B* **32**, 2625 (1985).
- [17] S. Manninen, V. Honkimäki, and P. Suortti, *J. Appl. Cryst.* **25**, 268 (1992).
- [18] V. Honkimäki, J. Sleight and P. Suortti, *J. Appl. Cryst.* **23**, 412 (1990).
- [19] V. Halonen, B. G. Williams, and T. Paakkari, *Phys. Fenn.* **10**, 107 (1974).
- [20] M. Y. Chou, M. L. Cohen, and S. T. Louie, *Phys. Rev. B* **33**, 6619 (1986).
- [21] L. Yongming, B. Johansson, and R. M. Nieminen, *J. Phys.: Condens. Matter* **3**, 1699 (1991).